
Article:
Hethcoat, M.G. orcid.org/0000-0002-5680-0635, Carreiras, J.M.B. orcid.org/0000-0003-2737-9420, Bryant, R.G. orcid.org/0000-0001-7943-4781 et al. (2 more authors) (2022) Combining Sentinel-1 and Landsat 8 does not improve classification accuracy of tropical selective logging. Remote Sensing, 14 (1). 179. ISSN 2072-4292

https://doi.org/10.3390/rs14010179

---

remote sensing

MDPI

Article

Combining Sentinel-1 and Landsat 8 Does Not Improve Classification Accuracy of Tropical Selective Logging

Matthew G. Hethcoat [1,2,3,*], João M. B. Carreiras [1,4], Robert G. Bryant [5], Shaun Quegan [1,4] and David P. Edwards [2]

1 Environmental Dynamics Group, School of Mathematics and Statistics, University of Sheffield, Sheffield S3 7RH, UK; j.carreiras@sheffield.ac.uk (J.M.B.C.); s.quegan@sheffield.ac.uk (S.Q.)
2 Ecology and Evolutionary Biology, School of Biosciences, University of Sheffield, Sheffield S10 2TN, UK; david.edwards@sheffield.ac.uk
3 Grantham Centre for Sustainable Futures, University of Sheffield, Sheffield S10 2TN, UK
4 National Centre for Earth Observation, University of Sheffield, Sheffield S3 7RH, UK
5 Department of Geography, University of Sheffield, Sheffield S3 7ND, UK; r.g.bryant@sheffield.ac.uk
* Correspondence: m.hethcoat@sheffield.ac.uk

Abstract: Tropical forests play a key role in the global carbon and hydrological cycles, maintaining biological diversity, slowing climate change, and supporting the global economy and local livelihoods. Yet, rapidly growing populations are driving continued degradation of tropical forests to supply wood products. The United Nations (UN) has developed the Reducing Emissions from Deforestation and Forest Degradation (REDD+) programme to mitigate climate impacts and biodiversity losses through improved forest management. Consistent and reliable systems are still needed to monitor tropical forests at large scales, however, degradation has largely been left out of most REDD+ reporting given the lack of effective monitoring and countries mainly focus on deforestation. Recent advances in combining optical data and Synthetic Aperture Radar (SAR) data have shown promise for improved ability to monitor forest losses, but it remains unclear if similar improvements could be made in detecting and mapping forest degradation. We used detailed selective logging records from three lowland tropical forest regions in the Brazilian Amazon to test the effectiveness of combining Landsat 8 and Sentinel-1 for selective logging detection. We built Random Forest models to classify pixel-based differences in logged and unlogged regions to understand if combining optical and SAR improved the detection capabilities over optical data alone. We found that the classification accuracy of models utilizing optical data from Landsat 8 alone were slightly higher than models that combined Sentinel-1 and Landsat 8. In general, detection of selective logging was high with both optical only and optical-SAR combined models, but our results show that the optical data was dominating the predictive performance and adding SAR data introduced noise, lowering the detection of selective logging. While we have shown limited capabilities with C-band SAR, the anticipated opening of the ALOS-PALSAR archives and the anticipated launch of NISAR and BIOMASS in 2023 should stimulate research investigating similar methods to understand if longer wavelength SAR might improve classification of areas affected by selective logging when combined with optical data.

Keywords: Brazil; degradation; forest disturbance; Grey Level Co-occurrence Matrix (GLCM); optical; random forest; reduced-impact logging; satellite; synthetic aperture radar; tropical forest

Citation: Hethcoat, M.G.; Carreiras, J.M.B.; Bryant, R.G.; Quegan, S.; Edwards, D.P. Combining Sentinel-1 and Landsat 8 Does Not Improve Classification Accuracy of Tropical Selective Logging. *Remote Sens.* **2022**, *14*, 179. https://doi.org/10.3390/rs14010179

Academic Editors: Fabio Gonçalves, Robert Treuhaft, Eben Broadbent and André Almeida

Received: 25 November 2021
Accepted: 30 December 2021
Published: 1 January 2022

1. Introduction

Tropical forests play a vital role in global carbon and hydrological cycling, maintaining biological diversity, mitigating climate change, and supporting the global economy and local livelihoods [1–4]. Rapidly growing populations and consumerism are driving continued loss and degradation of tropical forests to supply wood products, putting tremendous pressure on forests globally [5]. In recognizing these challenges, the United Nations (UN) has developed the Reducing Emissions from Deforestation and Forest Degradation (REDD+)

programme, which seeks to mitigate climate impacts and biodiversity losses through improved forest management practices [6]. To be eligible for REDD+ funding, developing countries must show progress toward reducing rates of degradation and deforestation. Yet, consistent and reliable systems are still needed to monitor tropical forests at large scales, with most REDD+ projects primarily focusing on deforestation because of the difficulties associated with monitoring degradation effectively [7].

Selective logging is often the first anthropogenic disturbance to affect primary forest cover and is an agent for additional changes, facilitating other forms of degradation and deforestation [8–11]. While selectively logged forests have increased microclimatic variability shortly after cutting [12], increased soil erosion [13,14], reduced tree diversity [15,16], altered forest phenology [17], and changed species compositions of fauna [18], forests subjected to selective logging generally maintain higher levels of biodiversity than other anthropogenic land-cover types, such as plantations or secondary forests [19]. Moreover, after accounting for the amount of wood removed, reduced impact logging (RIL) maintains higher biodiversity value than conventional selective logging (CL) practices [20], while simultaneously sequestering more carbon during regrowth [21]. Thus, in the context of REDD+ or alternative conservation initiatives, forests impacted by RIL offer high biodiversity value and carbon sequestration potential. Given that over 400 million hectares of tropical forest are estimated to be held for timber production [22], improved methods are needed to detect and monitor tropical selective logging activities to support national monitoring efforts to qualify for REDD+ funding.

Satellites offer the most cost-effective way to monitor forests for country-level reporting under REDD+. The technological capabilities to monitor tropical forests with satellite data have greatly improved over the last 10–15 years. Reliable deforestation alerts are available in near real-time from a number of organizations, including Global Forest Watch and the Brazilian National Institute for Space Research [23,24]. In contrast, detection and monitoring of forest degradation has lagged behind because of the complex and subtle disturbances associated with the selective harvesting of trees [25]. Recent advances in monitoring selective logging with optical data have shown promise in monitoring forest degradation [26–28], but the availability of optical data can be limited in regions with frequent cloud cover.

Synthetic Aperture Radar (SAR) data offers potential to advance detection of forest disturbances in regions with frequent cloud cover [29]. SAR satellites transmit radio waves and do not require solar illumination for data acquisition, enabling cloud penetration as well as data acquisition at night. SAR data have been used in forest mapping since the early 1990s (reviewed in [30]). Historically, the SAR data archives have been spatially and temporally inconsistent, with few programmes operating systematically to acquire global data. The Japanese Space Agency (JAXA) ALOS missions are an exception, but most of the data products are under commercial licenses and imagery costs over £1500 per scene. The launch of Sentinel-1A and -1B in 2014 and 2015, respectively, provided freely available C-band SAR data with global coverage every 5–12 days. This has spurred the development and use of dense time series of Sentinel-1 for detecting forest disturbances [29,31–33]. However, detecting and mapping selective logging in single Sentinel-1 scenes is insufficiently accurate across a range of logging intensities, and time series methods are needed [33].

A potential advance would be to develop methods that combine optical and SAR data to enhance detection of selective logging. Such combined methods have improved detection of small-scale deforestation [34–38]. However, it remains unclear if the recent advances in degradation detection and monitoring [26–28] could be improved by combining optical and SAR data. To date, no study has combined optical and SAR data to detect and map tropical selective logging. In addition, there has been no formal assessment of whether or not the accuracy of the results can be improved with such an approach. Here, we utilize optical and SAR data acquired over locations in Brazil to evaluate if combining Landsat 8 and Sentinel-1 improved detection of tropical selective logging. Landsat data on its own

has shown promising detection accuracy [27,28], and the question is whether adding the weak detection capabilities of SAR data [33] improves on this performance.

2. Study Area and Data

2.1. Field Data on Selective Logging

Selective logging data from three lowland, terra firme tropical forest regions in the Brazilian Amazon were used in this study (Figure 1); the Jacunda and Jamari regions, inside the Jacundá and Jamari National Forests, Rondônia, and the Saraca region, inside the Saracá-Taquera National Forest, Pará. Forest inventory data were provided by logging companies and covered 11 forest management units (FMUs) selectively logged between 2016 and 2017, comprising over 25,000 individual tree locations collected via GPS. FMUs were approximately 2000 ha each (mean: 2117, SD: 1057) and were managed with reduced-impact logging practices that included strict monitoring of logging activities and any impacts on the remaining forest. The logging intensity was calculated as the reported tree harvest, in cubic meters removed, per hectare for each FMU. Unlogged data from three additional locations, one inside each national forest (Jacunda, Jamari, and Saraca), comprised approximately 8000 randomly selected point locations known to have remained unlogged during the study period (Table 1).

Table 1. Data used in the classification of selective logging from eleven forest management units (FMUs) at three study regions in the Brazilian Amazon. All FMUs were managed with reduced-impact logging practices.

FMU	Logging Intensity (m^3 ha^{-1})	N (pixels)
Jacunda I 2016	6	2290
Jacunda I 2017	9	2822
Jacunda II 2016	10	1815
Jacunda II 2017	7	1310
Jacunda Unlogged	0	3000
Jamari I 2016	10	653
Jamari I 2017	12	911
Jamari III 2016	9	2058
Jamari III 2017	11	2597
Jamari Unlogged	0	1912
Saraca Ia 2017	12	3769
Saraca II 2016	25	3223
Saraca II 2017	21	4729
Saraca Unlogged	0	3000

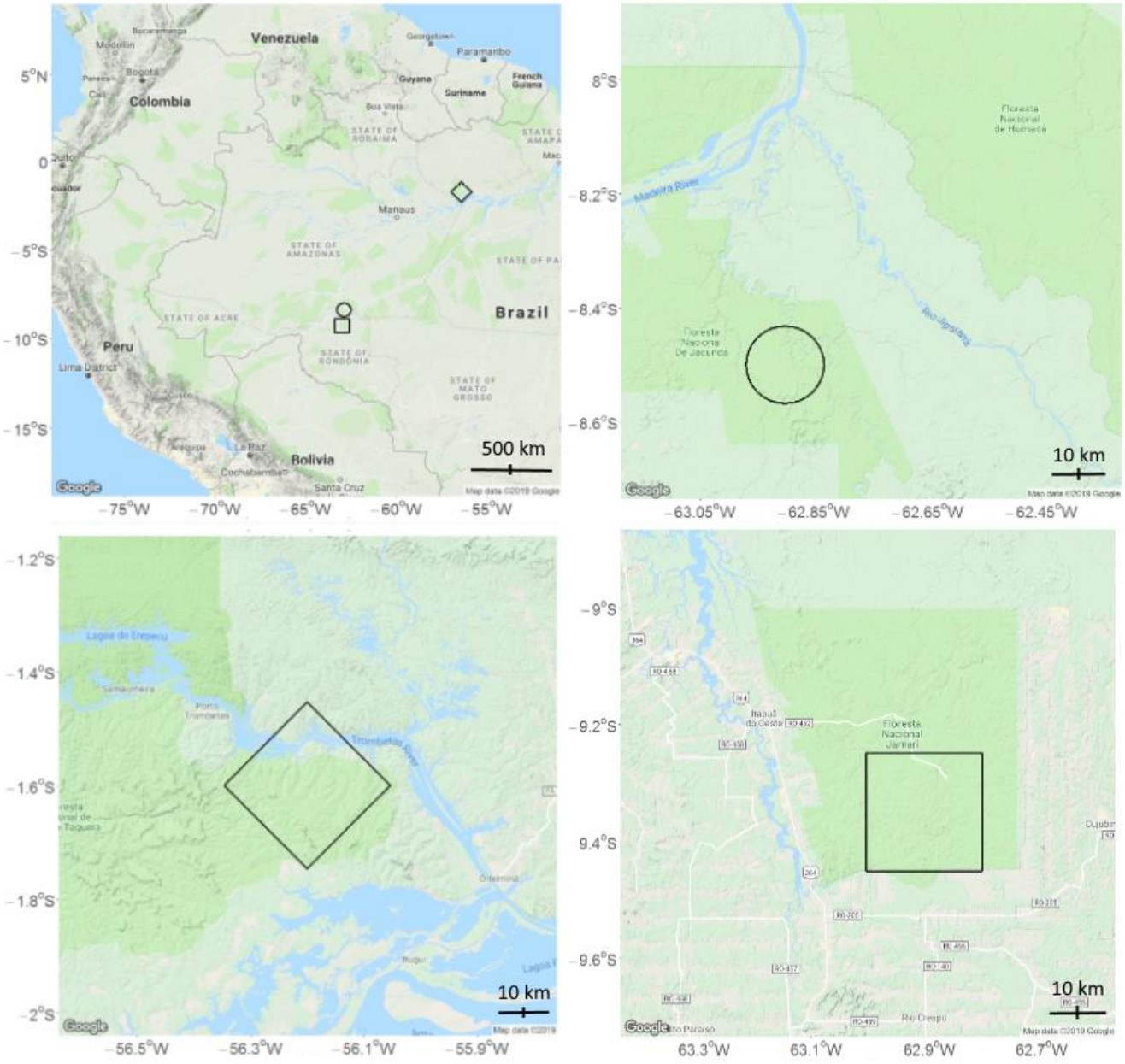

Figure 1. Location of the Jacunda (circle), Jamari (square), and Saraca (diamond) study regions in the Brazilian Amazon.

2.2. Satellite Data and Processing

The Landsat 8 and Sentinel-1 data archives were queried in Google Earth Engine (GEE) to obtain a single image over each FMU that was acquired late into the dry season logging period, but before the onset of the rainy season each year. This was to ensure that as many of the logging locations registered for that year's data had been logged, but that a cloud-free Landsat 8 image was still available. We chose to use Landsat 8 (over Sentinel-2) because we were building off of prior work focused on detecting logging from historical Landsat imagery [27,28]. In addition, it has been shown that no substantial difference exists in the logging detection capabilities between Landsat 8 and Sentinel-2 [39]. Thus, the marginal difference in spatial resolution (30 m with Landsat versus 20 with Sentinel-2) likely is of little importance here. In addition, while Sentinel-1 can penetrate clouds and thus a cloud-free scene is not required, backscatter can be affected by rainfall, surface water, and soil moisture [40]. Consequently, Sentinel-1 imagery was used within a similar time-frame

as the Landsat imagery at each site. A summary of image path, row, and acquisition date is in Table A1.

We used the Landsat 8 Surface Reflectance collection and the Sentinel-1 Ground Range Detected, Interferometric Wide mode (VV and VH) collection. In addition, we calculated a third band for all Sentinel-1 images as the ratio of the VV to the VH band (i.e., VV/VH). GEE calibrates and ortho-corrects Sentinel-1 imagery in the following steps using the Sentinel-1 Toolbox: (1) thermal noise removal; (2) radiometric calibration; and (3) geometric terrain correction (i.e., geocoding) using the Shuttle Radar Topography Mission (SRTM) 30 m digital elevation model (DEM). Furthermore, we (1) applied a radiometric slope correction in GEE detailed in [38]; (2) performed multi-temporal speckle filtering (using a median, 7 × 7 pixel window) detailed in [39]; and (3) reduced pixel resolution (via a mean) to produce 30 m pixels that aligned with Landsat 8 pixels at each location.

Given that forest disturbances from selective logging affect patches of forest and have associated canopy gaps, skid trails, etc., we calculated four Grey Level Co-occurrence Matrix (GLCM) metrics for each band in GEE. Prior work has shown that the use of GLCMs can result in spatial aggregation of forest disturbance predictions, resulting in over-estimation of disturbance with larger window sizes [27]. The choice of window size is thus a trade-off between increasing detection of forest disturbances while minimizing erroneous predictions. We chose a 5 × 5 window to calculate the Sum Average, Entropy, Contrast, and Angular Second Moment metrics [41], based on prior work indicating this size sufficiently balanced that trade-off [27]. The full dataset thus comprised a 45-element vector (6 Landsat surface reflectance bands, 3 SAR bands, 24 Landsat texture measures, and 12 SAR texture measures) for each pixel where logging occurred and the randomly selected pixels in an adjacent FMU that remained unlogged. The data were exported from GEE and collated in R version 4.0.2 for analyses.

3. Methods

3.1. Supervised Classification with Random Forest

We built Random Forest (RF) models using the randomForest package in program R version 4.0.2 [42]. The RF algorithm [43] is a machine-learning technique that uses an ensemble method to identify a response variable (here, whether a pixel was logged or unlogged) given a set of predictor variables (e.g., surface reflectance values). In contrast to a single decision tree, RF models employ multiple, independent decision trees. Random subsets of the training data are drawn, with replacement, to construct many trees in parallel, with each tree casting a vote for the class the input data should be assigned to. The withheld subset of the data (the out-of-bag fraction) can be used for validation in the absence of independent validation data [43]. To reduce generalization error, RF also uses a random subset of predictor variables in the decision at each node within a tree during construction.

We split the dataset into 90% for training and withheld 10% for validation. Moreover, we spatially filtered the training and validation datasets such that no observation from training was within 90 m of an observation within the validation dataset [28]. RF models have relatively few tuning parameters: The number of classification trees grown (ntree), and the number of predictor variables used to split a node into two sub-nodes (mtry). We performed a parameter optimization search to identify the combination of ntree (500–1000) and mtry (1–7) that minimized classification error of the out-of-bag (OOB) data. In practice, we iterated through combinations of ntree and mtry with RF in classification mode (i.e., class determined by a simple majority vote) to find the lowest OOB error for each training dataset—we did not restrict the size of samples drawn, depth of trees grown, or terminal node sizes and left them at their defaults (Table A2). Finally, once ntree and mtry were determined, we performed RF in probability mode (i.e., the proportion of votes from all trees that each observation was assigned to a particular class) and again used the OOB error to select the classification threshold (T) that maximized Cohen's kappa (k) during training of each model [44].

3.2. Model Validation

RF models were validated using a random subset of the full dataset (described in Section 3.1). By default, RF models assign an observation to the class indicated by the majority of decision trees [45]. However, the proportion of trees that assigned an observation to a particular class from the total set of trees can be obtained and a classification threshold (T) can be applied to this proportion [27,42]. The classification threshold (T) identified during model training (i.e., the value that maximized Cohen's Kappa in the out-of-bag data) was used to classify the validation dataset and a confusion matrix was generated. The confusion matrix then has the form:

		Reference	
		Logged	Unlogged
Predicted	Logged	D_L (True Positives)	D_{UL} (False Positives)
	Unlogged	N_L-D_L (False Negatives)	N_{UL}-D_{UL} (True Negatives)

where N_L and N_{UL} are the numbers of logged and unlogged observations in the validation dataset and D_L and D_{UL} are the numbers of logged and unlogged pixels detected as logged, respectively. We calculated the *detection rate* (DR):

$$DR = \frac{D_L}{N_L} \tag{1}$$

and *false alarm rate* (FAR):

$$FAR = \frac{D_{UL}}{N_{UL}} \tag{2}$$

as the frequencies that a logged or unlogged pixel was classified as logged, respectively. Thus, the DR is equivalent to 1 minus the omission error of the logged class and the FAR is the omission error of the unlogged class. In addition, we calculated the *false discovery rate* (FDR):

$$FDR = \frac{D_{UL}}{D_L + D_{UL}} \tag{3}$$

as the proportion of all observations that were detected as logged that were actually unlogged, which is equivalent to the commission error of the logged class (see [27] for further explanation) and the F_1-score:

$$F_1 = \frac{2\mathrm{TP}}{2\mathrm{TP} + \mathrm{FP} + \mathrm{FN}} \tag{4}$$

All measures were bias-corrected in line with best practices to account for the proportion of mapped classes [46].

4. Results

4.1. Landsat 8 Only

Random Forest performance for the model that used only Landsat 8 data is shown in Figure 2A. As the threshold value increased, the false alarm rate declined steeply and the detection rate stayed very high, indicating high proficiency at distinguishing logged observations. Overall, the final classification (Table 2) of selective logging was strong, with high detection, relatively low commission error, and high Kappa and F_1 scores.

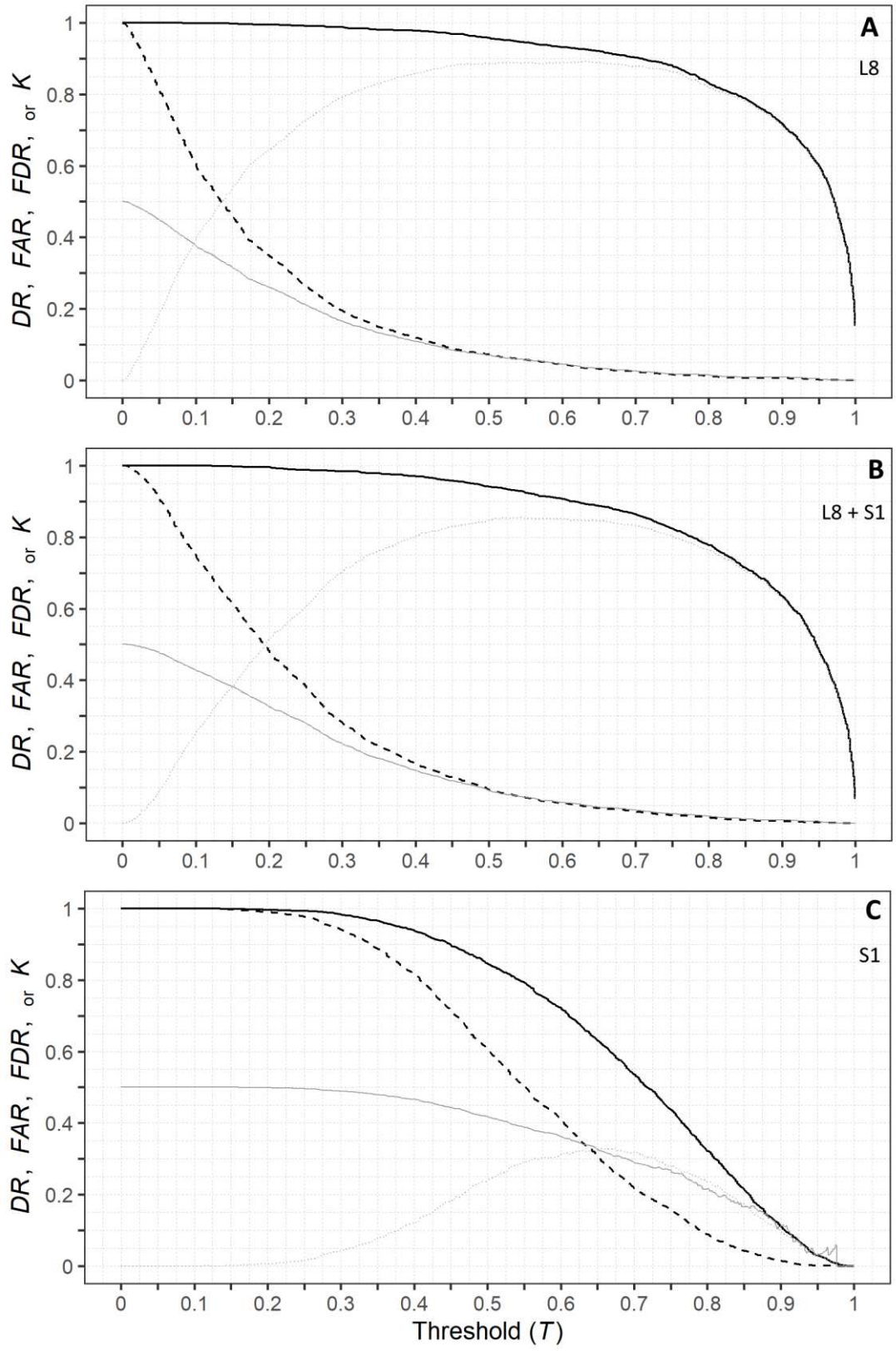

Figure 2. Random Forest model performance using data from only Landsat 8 (**A**), combined Landsat 8 (L8) and Sentinel-1 (**B**), and Sentinel-1 (S1) only (**C**). The detection rate and the false alarm rate are the solid and dashed black lines, respectively. The false discovery rate and Cohen's kappa are the solid and dashed grey lines, respectively.

Table 2. Summarized results from Random Forest model classification of logged and unlogged observations built with Landsat 8, combined Landsat 8 and Sentinel-1, and only Sentinel-1 data. The values if the classification threshold (T) and corresponding values of commission error for the logged and unlogged class (CE_L and CE_U, respectively), omission error for the logged and unlogged class (OE_L and OE_U, respectively), false discovery rate (FDR), detection rate (DR), Kappa (k), F_1 score (F_1), and overall accuracy (OA) are listed. Numbers are adjusted based on the proportion of mapped classes in Figure 3G,H,I [46].

Model	T	CE_L	CE_U	OE_L	OE_U	FDR	DR	k	F_1	OA
Landsat 8	0.508	5.9	3.5	14.3	1.3	5.9	85.6	0.8726	0.8967	96.08
Combined	0.527	7.0	5.4	17.2	2.0	7.0	82.8	0.8394	0.8762	94.29
Sentinel-1	0.632	34.7	35.7	92.3	2.4	34.7	7.7	0.0651	0.1385	64.34

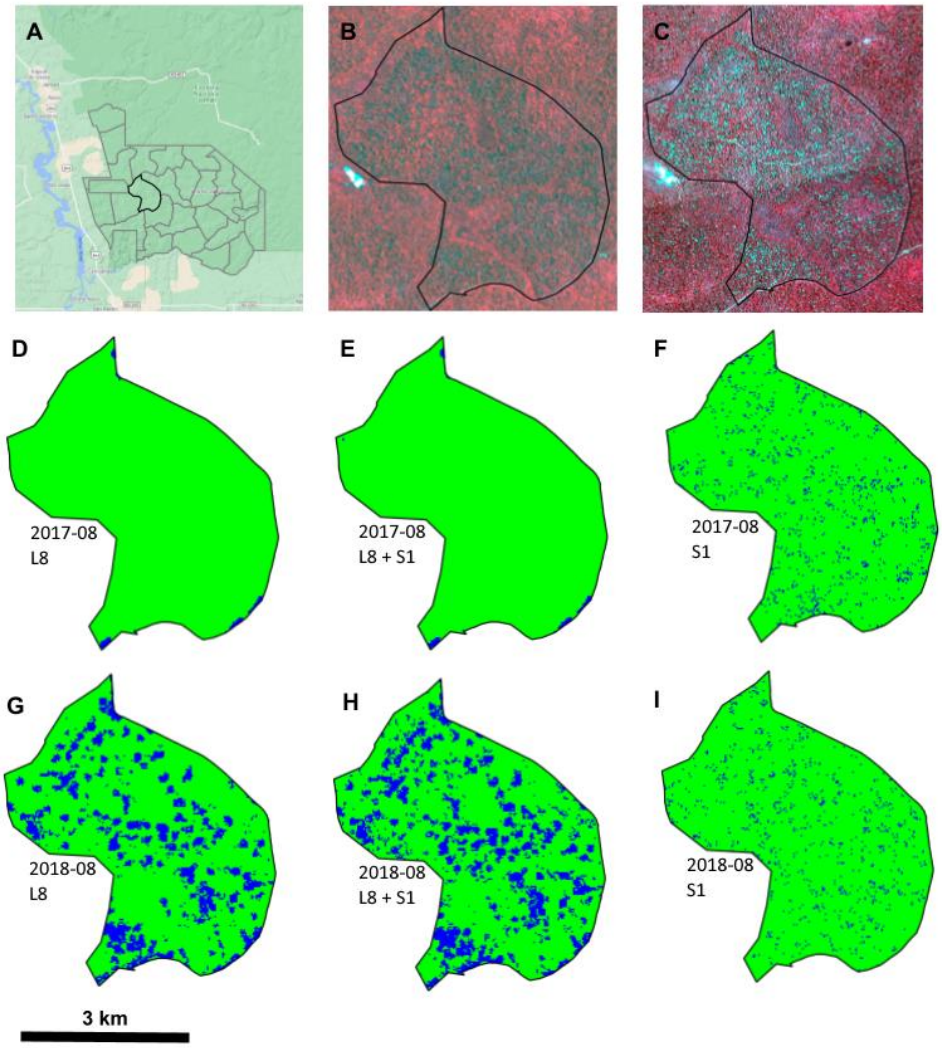

Figure 3. Area of selective logging in 2018 (outlined in black) within the Jamari National Forest, Rondônia, Brazil (**A**), Landsat 8 (L8) NIR,R,G imagery (30 m) from August 2018 (**B**), and PlanetScope NIR,R,G imagery (3 m) from October 2018 (**C**). Selective logging predictions from 2017 (i.e., one year before logging) are shown in blue for the Landsat 8 only model (**D**), the combined Landsat 8 and Sentinel-1 (S1) model (**E**), and Sentinel-1 only model (**F**). Selective logging predictions from 2018 (i.e., the year of logging) are shown in blue for the Landsat 8 only model (**G**), the combined Landsat 8 and Sentinel-1 model (**H**), and Sentinel-1 only model (**I**). Note, location data on cut trees was not known and the predictions of selective logging are for illustrative purposes and were not used for validation.

When the Landsat 8 only model was applied to a logging concession that lacked field data on cut tree locations, it was clear that the model performed quite well (Figure 3D,G). Almost no forest disturbance was detected in the year preceding logging (Figure 3D) while numerous forest disturbances were visible in the year of logging (Figure 3G).

4.2. Optical and SAR Combined

Performance of the RF model that used both Landsat 8 and Sentinel-1 is shown in Figure 2B. Again, the false alarm rate rapidly declined and the detection rate stayed very high as the threshold value increased. In general though, the detection rate declined slightly faster and the false alarm rate declined slightly slower in this combined model when compared to the Landsat only model (Table 2), suggesting greater difficulty distinguishing logged and unlogged observations. Overall, the results with the combined model indicate no improvement in classification of selective logging and the SAR data adds uncertainty to the classification, slightly increasing both commission and omission errors (Table 2).

When the combined Landsat 8 and Sentinel-1 model was applied to the same logging concession that lacked field data on cut tree locations, the results were very similar to those of the Landsat only model (Figure 3G,H). Again, almost no forest disturbance was detected in the year preceding logging (Figure 3E) and numerous forest disturbances are visible in the year of logging (Figure 3H), with the addition of some detections (speckled in areas not mapped in Figure 3G). Overall, these findings suggest that Sentinel-1 offers little extra information within a supervised classification scheme and the Landsat data were driving the classification results (Figure A1).

4.3. Sentinel-1 Only

Performance of the RF model that only used Sentinel-1 data is shown in Figure 2C for completeness. The false alarm and detection rates gradually declined as the threshold value increased, with the rates declining roughly in parallel, indicating significant difficulty in distinguishing logged and unlogged observations (Table 2). When this model was applied to the same logging concession lacking location data for trees cut, forest disturbances were randomly speckled in the year preceding logging (Figure 3F) and the year of logging (Figure 3I). Overall, these findings suggest that the Sentinel-1 data were too noisy for supervised classification of selective logging.

5. Discussion

We have shown that combining C-band SAR from Sentinel-1 and optical data from Landsat 8 did not offer a performance advantage over simply using optical data to detect tropical selective logging (TSL) in single images. Prior studies have shown an improvement in deforestation monitoring by combining optical and SAR [34,35,38,47,48]. For example, Hirschmugl et al. [38] showed very good results when combining SAR and optical data, however, their approach employed multi-step time series methods for each data type and they focused on small scale deforestation, not selective logging. It should also be noted that our study sites were managed under reduced-impact logging practices, with most of the logging records being of relatively low intensity (Table 1) and only 2 sites were close to the legal limit allowed within the Amazon (30 m^3 ha^{-1}). While single-image classification of selective logging with Sentinel-1 data has been shown to perform poorly, even when restricted to the most intensively logged regions [33], it is still possible that different regions with either higher logging intensities, conventional logging practices, or more pervasive cloud-cover might benefit from synergistic use of C-band SAR and optical imagery.

The Sentinel-1 data used here were spatially averaged, from 10 m to 30 m, to align with Landsat 8. We anticipated some increase in the detection of TSL resulting from reduction of speckle and an increase in the signal-to-noise ratio of the SAR data [49]. However, our results are in line with previous research which demonstrated that even heavily processed SAR data (e.g., through use of adaptive temporal filters for speckle reduction) are too noisy for supervised classification of single-image SAR data across a range of wavelengths [33].

Indeed, those data were used at full resolution (i.e., not spatially averaged to align with Landsat 8 pixels) and included much more training data on logging, yet the results were generally similar to those outlined here. Therefore, it seems consistent that single-image C-band SAR data signal-to-noise ratio precludes effective supervised classification of TSL, and either a well-constrained temporal component [29] or deep learning [50] might be needed within the workflow to effectively detect and track subtle forest disturbances.

Recent analyses have shown strong detection of forest degradation with a time series analysis of Landsat data [26]. In general, there has been an increasing trend in the use of time series methods to monitor forest disturbances [29,33,35,38,48,51,52] that is likely to continue, given the growing availability of Earth observation data [53]. A form of single image analysis that relies on summarizing a single image in relation to a temporal component of the data stream is a simple starting point and already viable [29,32,48,54]. Our results, and the continued development of newer time series methods, should stimulate research looking to combine optical and SAR data into a joint or multivariate time-series approach [55,56]. While dense time series of historical SAR data are not currently available, such an approach could be used in near-real-time analyses or to develop alert systems that combine Landsat, Sentinel-2 and Sentinel-1 data.

6. Conclusions

Improving current abilities to detect and map tropical selective logging is essential for understanding the impacts on global biodiversity, and tracking and mitigating the climate implications of forest degradation. Yet, large uncertainties remain in understanding the full impacts of selective logging because the advances in detection and monitoring at large spatial scales are only just emerging [27,28,57,58]. Such progress would enable the mapping of primary forest as well as identify logged regions that possess high conservation value. Tropical forests store an immense amount of carbon and quantifying the extent of forest degradation from selective logging is a key step in refining our understanding of the terrestrial portion of the carbon budget [1,59,60].

To better protect tropical forest carbon stocks, investment in REDD+ is anticipated to reach USD 30 billion annually [61]. In addition, Reduced-Impact Logging (RIL) techniques, that emphasize reducing carbon emissions (RIL-C), have been suggested as a tool to incentivize voluntary carbon markets [62]. However, a lack of emissions verification systems, because of the difficulty in monitoring logging, has limited the adoption of these practices [62]. Fortunately, while large-scale and real-time monitoring of forest degradation has remained an elusive goal to date, the speed and momentum of advances have accelerated in recent years. The next challenge will likely be creating successful linkages between technical and political domains so that advances in remote sensing effectively inform complex governmental and international frameworks that have been established to protect and monitor tropical forests.

Author Contributions: Conceptualization, M.G.H., J.M.B.C., R.G.B., S.Q. and D.P.E.; methodology, M.G.H., J.M.B.C., R.G.B., S.Q. and D.P.E.; formal analysis, M.G.H.; writing—original draft preparation, M.G.H.; writing—review and editing, M.G.H., J.M.B.C., R.G.B., S.Q. and D.P.E.; visualization, M.G.H.; supervision, J.M.B.C., R.G.B., S.Q. and D.P.E.; funding acquisition, J.M.B.C., R.G.B., S.Q. and D.P.E. All authors have read and agreed to the published version of the manuscript.

Funding: M.G.H. was funded by the Grantham Centre for Sustainable Futures. J.M.B.C. was funded by the Natural Environment Research Council (Agreement PR140015 between NERC and the National Centre for Earth Observation).

Institutional Review Board Statement: Not Application.

Informed Consent Statement: Not Application.

Data Availability Statement: Not Application.

Acknowledgments: We would like to thank AMATA Brazil for providing access to logging records for Jamari and logistical support. We would also like to thank the Google Earth Engine developers and community for access to the datasets that made this work possible, as well as Planet for access to high resolution imagery through the education and research program.

Conflicts of Interest: The authors declare no conflict of interest. The funders had no role in the design of the study; in the collection, analyses, or interpretation of data; in the writing of the manuscript, or in the decision to publish the results.

Appendix A

Table A1. Satellite imagery acquisition dates over the forest management units (FMU) in the Brazilian Amazon used in Random Forest classification of selective logging.

FMU Name	Landsat 8 PathRow_Date	Sentinel-1 Date
Jacunda_I_2016	232066_20160920	20161012
Jacunda_I_2017	232066_20170907	20170901
Jacunda_II_2016	232066_20160920	20161012
Jacunda_II_2017	232066_20170907	20170913
Jacunda_UNL	232066_20160803	20160930
	232066_20170806	20170901
Jamari_I_2016	232066_20160819	20160930
Jamari_I_2017	232066_20170923	20170925
Jamari_III_2016	232066_20160803	20161012
Jamari_III_2017	232066_20170907	20170913
Jamari_UNL	232066_20160803	20161012
	232066_20170907	20170925
Saraca_Ia_2017	229061_20171105	20170927
Saraca_II_2016	228061_20161111	20170822
Saraca_II_2017	228061_20170911	20170822
Saraca_UNL	228061_20161111	20161002
	228061_20170911	20170927

Table A2. Parameter optimization results for the number of trees (*ntree*) and the number of variables used at each node (*mtry*) that minimized the out-of-bag classification error during training of each model.

mTry	nTree	Model
3	700	Landsat 8
3	700	Combined
1	800	Sentinel-1

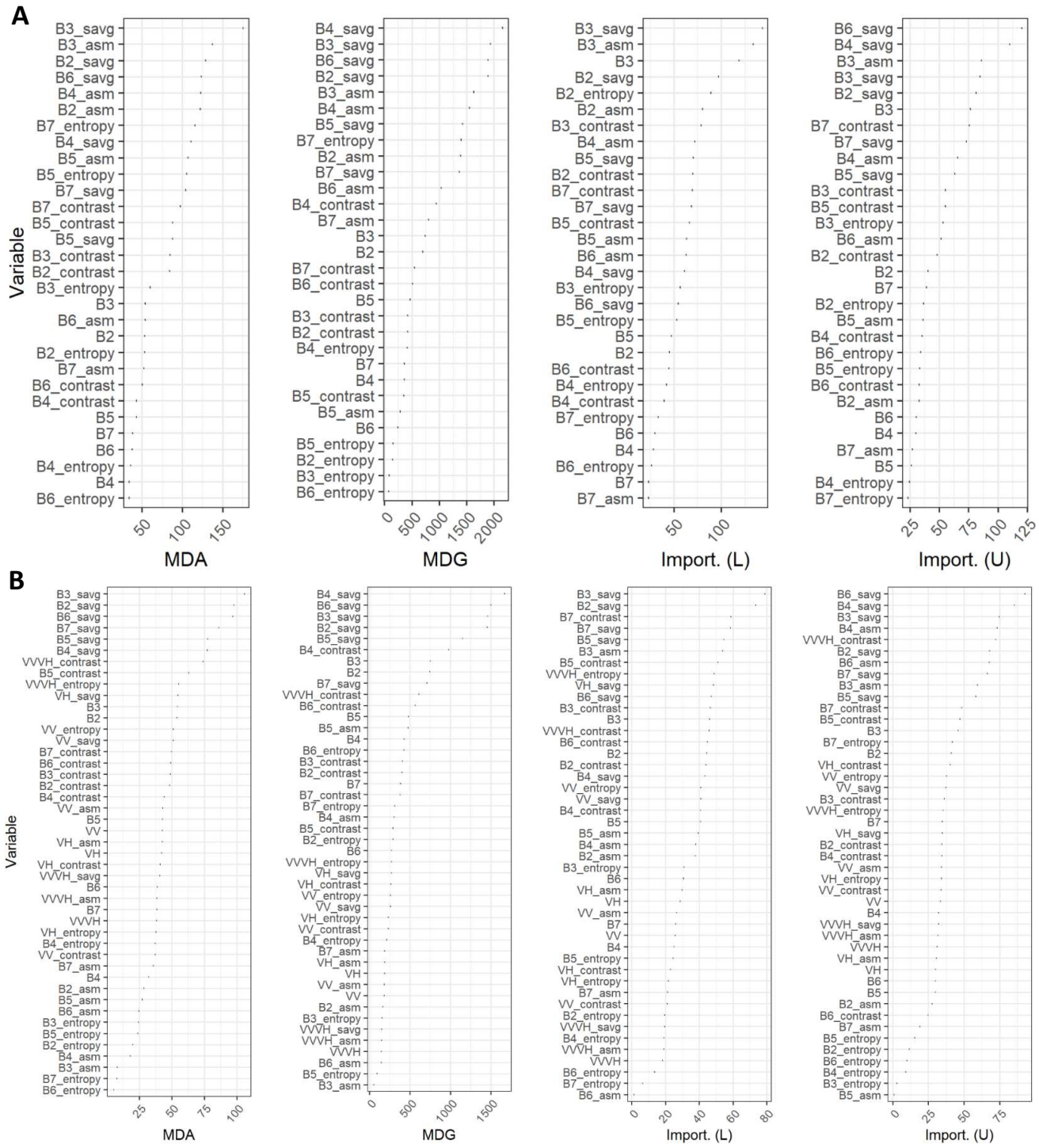

Figure A1. Variable importance for Random Forest model that used only Landsat 8 (**A**) and combined Landsat 8 and Sentinel-1 (**B**), with Mean Decrease in Accuracy (MDA), Mean Decrease in Gini (MDG), and Importance measures for classifying logged and unlogged observations (Import. L and Import. U, respectively).

References

1. Baccini, A.; Walker, W.; Carvalho, L.; Farina, M.; Sulla-Menashe, D.; Houghton, R.A. Tropical forests are a net carbon source based on aboveground measurements of gain and loss. *Science* **2017**, *358*, 230–234. [CrossRef]
2. Barlow, J.; Lennox, G.D.; Ferreira, J.; Berenguer, E.; Lees, A.C.; Mac Nally, R.; Thomson, J.R.; Ferraz, S.F.D.B.; Louzada, J.; Oliveira, V.H.F.; et al. Anthropogenic disturbance in tropical forests can double biodiversity loss from deforestation. *Nature* **2016**, *535*, 144–147. [CrossRef]

3. Lewis, S.L.; Maslin, M.A. Defining the Anthropocene. *Nature* **2015**, *519*, 171–180. [CrossRef] [PubMed]
4. Pan, Y.D.; Birdsey, R.A.; Fang, J.Y.; Houghton, R.; Kauppi, P.E.; Kurz, W.A.; Phillips, O.L.; Shvidenko, A.; Lewis, S.L.; Canadell, J.G.; et al. A Large and Persistent Carbon Sink in the World's Forests. *Science* **2011**, *333*, 988–993. [CrossRef] [PubMed]
5. Edwards, D.P.; Socolar, J.B.; Mills, S.C.; Burivalova, Z.; Koh, L.P.; Wilcove, D.S. Conservation of Tropical Forests in the Anthropocene. *Curr. Biol.* **2019**, *29*, R1008–R1020. [CrossRef] [PubMed]
6. Team, F. GOFC-GOLD. A Sourcebook of Methods and Procedures for Monitoring Essential Biodiversity Variables in Tropical Forests with Remote Sensing. 2017. Available online: https://ec.europa.eu/jrc/en/publication/gofc-gold-2017-sourcebook-methods-and-procedures-monitoring-essential-biodiversity-variables (accessed on 13 February 2021).
7. Milbank, C.; Coomes, D.; Vira, B. Assessing the Progress of REDD+ Projects towards the Sustainable Development Goals. *Forests* **2018**, *9*, 589. [CrossRef]
8. Nepstad, D.C.; Verssimo, A.; Alencar, A.; Nobre, C.; Lima, E.; Lefebvre, P.; Schlesinger, P.; Potter, C.; Moutinho, P.; Mendoza, E.; et al. Large-scale impoverishment of Amazonian forests by logging and fire. *Nature* **1999**, *398*, 505–508. [CrossRef]
9. Asner, G.P.; Knapp, D.E.; Broadbent, E.N.; Oliveira, P.J.C.; Keller, M.; Silva, J.N. Selective Logging in the Brazilian Amazon. *Science* **2005**, *310*, 480–482. [CrossRef]
10. Asner, G.P.; Broadbent, E.N.; Oliveira, P.J.C.; Keller, M.; Knapp, D.E.; Silva, J.N.M. Condition and fate of logged forests in the Brazilian Amazon. *Proc. Natl. Acad. Sci. USA* **2006**, *103*, 12947–12950. [CrossRef]
11. Asner, G.P.; Keller, M.; Lentini, M.; Merry, F.; Souza, C. Selective Logging and Its Relation to Deforestation. In *Amazonia and Global Change*; Keller, M., Bustamante, M., Gash, J., Dias, P.S., Eds.; American Geophysical Union: Washington, DC, USA, 2009; pp. 25–42.
12. Stratford, J.A.; Robinson, W.D. Gulliver Travels to the Fragmented Tropics: Geographic Variation in Mechanisms of Avian Extinction. *Front. Ecol. Environ.* **2005**, *3*, 85–92. [CrossRef]
13. Douglas, I. Hydrological investigations of forest disturbance and land cover impacts in South–East Asia: A review. *Philos. Trans. R. Soc. B Biol. Sci.* **1999**, *354*, 1725–1738. [CrossRef]
14. Hartanto, H.; Prabhu, R.; Widayat, A.S.; Asdak, C. Factors affecting runoff and soil erosion: Plot-level soil loss monitoring for assessing sustainability of forest management. *For. Ecol. Manag.* **2003**, *180*, 361–374. [CrossRef]
15. Berry, N.J.; Phillips, O.; Ong, R.C.; Hamer, K.C. Impacts of selective logging on tree diversity across a rainforest landscape: The importance of spatial scale. *Landsc. Ecol.* **2008**, *23*, 915–929. [CrossRef]
16. Martin, P.A.; Newton, A.C.; Pfeifer, M.; Khoo, M.; Bullock, J.M. Impacts of tropical selective logging on carbon storage and tree species richness: A meta-analysis. *For. Ecol. Manag.* **2015**, *356*, 224–233. [CrossRef]
17. Koltunov, A.; Ustin, S.L.; Asner, G.; Fung, I. Selective logging changes forest phenology in the Brazilian Amazon: Evidence from MODIS image time series analysis. *Remote Sens. Environ.* **2009**, *113*, 2431–2440. [CrossRef]
18. Burivalova, Z.; Şekercioğlu, Ç.H.; Koh, L.P. Thresholds of Logging Intensity to Maintain Tropical Forest Biodiversity. *Curr. Biol.* **2014**, *24*, 1893–1898. [CrossRef] [PubMed]
19. Edwards, D.P.; Tobias, J.; Sheil, D.; Meijaard, E.; Laurance, W.F. Maintaining ecosystem function and services in logged tropical forests. *Trends Ecol. Evol.* **2014**, *29*, 511–520. [CrossRef]
20. Bicknell, J.E.; Struebig, M.; Edwards, D.P.; Davies, Z.G. Improved timber harvest techniques maintain biodiversity in tropical forests. *Curr. Biol.* **2014**, *24*, R1119–R1120. [CrossRef] [PubMed]
21. Putz, F.; Sist, P.; Fredericksen, T.; Dykstra, D. Reduced-impact logging: Challenges and opportunities. *For. Ecol. Manag.* **2008**, *256*, 1427–1433. [CrossRef]
22. Blaser, J.; Sarre, A.; Poore, D.; Johnson, S. *Status of Tropical Forest Management 2011. ITTO Technical Series No 38*; International Tropical Timber Organization: Yokohama, Japan, 2011.
23. Hansen, M.C.; Potapov, P.V.; Moore, R.; Hancher, M.; Turubanova, S.A.; Tyukavina, A.; Thau, D.; Stehman, S.V.; Goetz, S.J.; Loveland, T.R.; et al. High-resolution global maps of 21st-century forest cover change. *Science* **2013**, *342*, 850–853. [CrossRef]
24. Diniz, C.G.; De Souza, A.A.A.; Santos, D.C.; Dias, M.C.; Luz, N.; De Moraes, D.R.V.; Maia, J.S.A.; Gomes, A.R.; Narvaes, I.D.S.; Valeriano, D.M.; et al. DETER-B: The New Amazon Near Real-Time Deforestation Detection System. *IEEE J. Sel. Top. Appl. Earth Obs. Remote Sens.* **2015**, *8*, 3619–3628. [CrossRef]
25. Ghazoul, J.; Burivalova, Z.; Garcia-Ulloa, J.; King, L.A. Conceptualizing Forest Degradation. *Trends Ecol. Evol.* **2015**, *30*, 622–632. [CrossRef] [PubMed]
26. Bullock, E.L.; Woodcock, C.E.; Olofsson, P. Monitoring tropical forest degradation using spectral unmixing and Landsat time series analysis. *Remote. Sens. Environ.* **2018**, *238*, 110968. [CrossRef]
27. Hethcoat, M.; Edwards, D.; Carreiras, J.; Bryant, R.; França, F.; Quegan, S. A machine learning approach to map tropical selective logging. *Remote. Sens. Environ.* **2019**, *221*, 569–582. [CrossRef]
28. Hethcoat, M.G.; Carreiras, J.M.B.; Edwards, D.; Bryant, R.G.; Peres, C.A.; Quegan, S. Mapping pervasive selective logging in the south-west Brazilian Amazon 2000–2019. *Environ. Res. Lett.* **2020**, *15*, 094057. [CrossRef]
29. Reiche, J.; Mullissa, A.; Slagter, B.; Gou, Y.; Tsendbazar, N.-E.; Odongo-Braun, C.; Vollrath, A.; Weisse, M.J.; Stolle, F.; Pickens, A.; et al. Forest disturbance alerts for the Congo Basin using Sentinel-1. *Environ. Res. Lett.* **2021**, *16*, 024005. [CrossRef]
30. Koch, B. Status and future of laser scanning, synthetic aperture radar and hyperspectral remote sensing data for forest biomass assessment. *ISPRS J. Photogramm. Remote Sens.* **2010**, *65*, 581–590. [CrossRef]

31. Reiche, J.; De Bruin, S.; Hoekman, D.; Verbesselt, J.; Herold, M. A Bayesian Approach to Combine Landsat and ALOS PALSAR Time Series for Near Real-Time Deforestation Detection. *Remote Sens.* **2015**, *7*, 4973–4996. [CrossRef]
32. Reiche, J.; Verhoeven, R.; Verbesselt, J.; Hamunyela, E.; Wielaard, N.; Herold, M. Characterizing Tropical Forest Cover Loss Using Dense Sentinel-1 Data and Active Fire Alerts. *Remote Sens.* **2018**, *10*, 777. [CrossRef]
33. Hethcoat, M.G.; Carreiras, J.M.; Edwards, D.P.; Bryant, R.G.; Quegan, S. Detecting tropical selective logging with C-band SAR data may require a time series approach. *Remote Sens. Environ.* **2021**, *259*, 112411. [CrossRef]
34. Laurin, G.V.; Liesenberg, V.; Chen, Q.; Guerriero, L.; Del Frate, F.; Bartolini, A.; Coomes, D.; Wilebore, B.; Lindsell, J.; Valentini, R. Optical and SAR sensor synergies for forest and land cover mapping in a tropical site in West Africa. *Int. J. Appl. Earth Obs. Geoinf.* **2013**, *21*, 7–16. [CrossRef]
35. Reiche, J.; Verbesselt, J.; Hoekman, D.; Herold, M. Fusing Landsat and SAR time series to detect deforestation in the tropics. *Remote Sens. Environ.* **2015**, *156*, 276–293. [CrossRef]
36. Joshi, N.; Baumann, M.; Ehammer, A.; Fensholt, R.; Grogan, K.; Hostert, P.; Jepsen, M.R.; Kuemmerle, T.; Meyfroidt, P.; Mitchard, E.T.A.; et al. A Review of the Application of Optical and Radar Remote Sensing Data Fusion to Land Use Mapping and Monitoring. *Remote Sens.* **2016**, *8*, 70. [CrossRef]
37. Mercier, A.; Betbeder, J.; Rumiano, F.; Baudry, J.; Gond, V.; Blanc, L.; Bourgoin, C.; Cornu, G.; Ciudad, C.; Marchamalo, M.; et al. Evaluation of Sentinel-1 and 2 Time Series for Land Cover Classification of Forest–Agriculture Mosaics in Temperate and Tropical Landscapes. *Remote Sens.* **2019**, *11*, 979. [CrossRef]
38. Hirschmugl, M.; Deutscher, J.; Sobe, C.; Bouvet, A.; Mermoz, S.; Schardt, M. Use of SAR and Optical Time Series for Tropical Forest Disturbance Mapping. *Remote Sens.* **2020**, *12*, 727. [CrossRef]
39. Lima, T.A.; Beuchle, R.; Langner, A.; Grecchi, R.C.; Griess, V.C.; Achard, F. Comparing Sentinel-2 MSI and Landsat 8 OLI Imagery for Monitoring Selective Logging in the Brazilian Amazon. *Remote Sens.* **2019**, *11*, 961. [CrossRef]
40. Flores-Anderson, A.I.; Herndon, K.E.; Thapa, R.B.; Cherrington, E. (Eds.) *The SAR Handbook: Comprehensive Methodologies for Forest Monitoring and Biomass Estimation*; NASA: Washington, DC, USA, 2019.
41. Haralick, R.M.; Shanmugam, K.; Dinstein, I. Textural Features for Image Classification. *IEEE Trans. Syst. Man Cybern.* **1973**, *3*, 610–621. [CrossRef]
42. Liaw, A.; Wiener, M. Classification and Regression by Random. *Forest* **2002**, *2*, 5.
43. Breiman, L. Random Forests. *Mach. Learn.* **2001**, *45*, 5–32. [CrossRef]
44. Cohen, J. A Coefficient of Agreement for Nominal Scales. *Educ. Psychol. Meas.* **1960**, *20*, 37–46. [CrossRef]
45. Breiman, L. Statistical Modeling: The Two Cultures. *Stat. Sci.* **2001**, *16*, 199–231. [CrossRef]
46. Olofsson, P.; Foody, G.M.; Herold, M.; Stehman, S.V.; Woodcock, C.E.; Wulder, M.A. Good practices for estimating area and assessing accuracy of land change. *Remote Sens. Environ.* **2014**, *148*, 42–57. [CrossRef]
47. Erasmi, S.; Twele, A. Regional land cover mapping in the humid tropics using combined optical and SAR satellite data—a case study from Central Sulawesi, Indonesia. *Int. J. Remote Sens.* **2009**, *30*, 2465–2478. [CrossRef]
48. Reiche, J.; Hamunyela, E.; Verbesselt, J.; Hoekman, D.; Herold, M. Improving near-real time deforestation monitoring in tropical dry forests by combining dense Sentinel-1 time series with Landsat and ALOS-2 PALSAR-2. *Remote Sens. Environ.* **2018**, *204*, 147–161. [CrossRef]
49. Quegan, S.; Yu, J.J. Filtering of multichannel SAR images. *IEEE Trans. Geosci. Remote Sens.* **2001**, *39*, 2373–2379. [CrossRef]
50. Kuck, T.N.; Sano, E.E.; Bispo, P.D.C.; Shiguemori, E.H.; Filho, P.F.F.S.; Matricardi, E.A.T. A Comparative Assessment of Machine-Learning Techniques for Forest Degradation Caused by Selective Logging in an Amazon Region Using Multitemporal X-Band SAR Images. *Remote Sens.* **2021**, *13*, 3341. [CrossRef]
51. Bouvet, A.; Mermoz, S.; Ballère, M.; Koleck, T.; Le Toan, T. Use of the SAR Shadowing Effect for Deforestation Detection with Sentinel-1 Time Series. *Remote Sens.* **2018**, *10*, 1250. [CrossRef]
52. Ballère, M.; Bouvet, A.; Mermoz, S.; Le Toan, T.; Koleck, T.; Bedeau, C.; André, M.; Forestier, E.; Frison, P.-L.; Lardeux, C. SAR data for tropical forest disturbance alerts in French Guiana: Benefit over optical imagery. *Remote Sens. Environ.* **2021**, *252*, 112159. [CrossRef]
53. Finer, M.; Novoa, S.; Weisse, M.J.; Petersen, R.; Mascaro, J.; Souto, T.; Stearns, F.; Martinez, R.G. Combating deforestation: From satellite to intervention. *Science* **2018**, *360*, 1303–1305. [CrossRef]
54. Koeniguer, E.C.; Nicolas, J.-M. Change Detection Based on the Coefficient of Variation in SAR Time-Series of Urban Areas. *Remote Sens.* **2020**, *12*, 2089. [CrossRef]
55. Prendes, J.; Chabert, M.; Pascal, F.; Giros, A.; Tourneret, J.-Y. A New Multivariate Statistical Model for Change Detection in Images Acquired by Homogeneous and Heterogeneous Sensors. *IEEE Trans. Image Process.* **2015**, *24*, 799–812. [CrossRef] [PubMed]
56. Cardille, J.A.; Perez, E.; Crowley, M.A.; Wulder, M.A.; White, J.C.; Hermosilla, T. Multi-sensor change detection for within-year capture and labelling of forest disturbance. *Remote Sens. Environ.* **2021**, *268*, 112741. [CrossRef]
57. Langner, A.; Miettinen, J.; Kukkonen, M.; Vancutsem, C.; Simonetti, D.; Vieilledent, G.; Verhegghen, A.; Gallego, J.; Stibig, H.-J. Towards Operational Monitoring of Forest Canopy Disturbance in Evergreen Rain Forests: A Test Case in Continental Southeast Asia. *Remote Sens.* **2018**, *10*, 544. [CrossRef]
58. Vancutsem, C.; Achard, F.; Pekel, J.-F.; Vieilledent, G.; Carboni, S.; Simonetti, D.; Gallego, J.; Aragão, L.E.O.C.; Nasi, R. Long-term (1990–2019) monitoring of forest cover changes in the humid tropics. *Sci. Adv.* **2021**, *7*, eabe1603. [CrossRef] [PubMed]
59. Mitchard, E.T.A. The tropical forest carbon cycle and climate change. *Nature* **2018**, *559*, 527–534. [CrossRef]

60. Friedlingstein, P.; Jones, M.W.; O'Sullivan, M.; Andrew, R.M.; Bakker, D.C.E.; Hauck, J.; Le Quéré, C.; Peters, G.P.; Peters, W.; Pongratz, J.; et al. Global Carbon Budget 2021. *Earth Syst. Sci. Data Discuss.* **2020**, *4*, 3269—3340. [CrossRef]
61. Phelps, J.; Webb, E.L.; Agrawal, A. Does REDD+ Threaten to Recentralize Forest Governance? *Science* **2010**, *328*, 312–313. [CrossRef]
62. Ellis, P.W.; Gopalakrishna, T.; Goodman, R.C.; Putz, F.E.; Roopsind, A.; Umunay, P.M.; Zalman, J.; Ellis, E.A.; Mo, K.; Gregoire, T.G.; et al. Reduced-impact logging for climate change mitigation (RIL-C) can halve selective logging emissions from tropical forests. *For. Ecol. Manag.* **2019**, *438*, 255–266. [CrossRef]